Available online at www.sciencedirect.com
SCIENCE DIRECT®
Journal of the European Ceramic Society 25 (2005) 1581–1589
www.elsevier.com/locate/jeurceramsoc

Laser stereolithography of ZrO_2 toughened Al_2O_3

A. Licciulli [a,*], C. Esposito Corcione [a], A. Greco [a], V. Amicarelli [b], A. Maffezzoli [a]

[a] *Dipartimento di Ingegneria dell'innovazione, Università degli Studi di Lecce, Campus Universitario, Via per Arnesano 73100 Lecce, Italy*
[b] *Dipartimento di Ingegneria Civile ed Ambientale, Politecnico di bari, Bari, Italy*

Received 3 February 2003; received in revised form 1 December 2003; accepted 8 December 2003
Available online 3 August 2004

Abstract

Ceramic laser stereolithography is a manufacturing process suitable candidate for the production of complex shape technical ceramics. The green ceramic is produced layer by layer through laser polymerisation of UV curable ceramic suspensions. A number of critical issues deserve attention: high solid loading and low viscosity of the suspensions, high UV reactivity, prevention of interlayer delamination in the green and in the sintered body, good mechanical performance. In this work, ZrO_2 reinforced Al_2O_3 components have been obtained from an acrylic modified zircon loaded with alumina powders. The zircon compound is effective as organic photoactivated resin and allows the dispersion of a high volume fraction of Al_2O_3 powder (up to 50 vol.%) while keeping viscosity at reasonable low values. The zircon compound also represents a liquid ceramic precursor that converts to oxide after burning out of the binder. Thanks to the good dispersion of the alumina powder in the zircon acrylate, a uniform dispersion of ZrO_2 submicron particles is obtained after pyrolysis. These are located at the grain boundaries between alumina grains. Formation of both monoclinic and tetragonal ZrO_2 occurs as evidenced by XRD. No delamination occurs in bending tests as evidenced by SEM fractography, satisfactory modulus and strength values were concurrently found.

Keywords: Stereolithography; Precursors-organic: Al_2O_3, ZrO_2

1. Introduction

Over the last decade, several solid free form fabrication (SFF) methods have been investigated as techniques to produce polymer, metal or ceramic prototypes components directly from computer 3D drawings.[1] In particular, solid free form fabrication of ceramics should produce near net-shape structural[2–4] and/or functional[5,6] ceramic parts by additive methods on a layer by layer basis. To some extent, the term prototype in the case of ceramics manufacturing is misleading since useful objects, functional testing tools, or pre-production series are intended to be produced. The interest in this fabrication process arises in different applications: ceramic materials are needed as prototypes for functional tests and pre-series production tests, ceramic moulds in single units are needed in metal casting, e.g., jewellery, ceramic cores are needed in investment casting of hollow objects. Ceramics are good biomaterials: implants with inert or bioactive and reabsorbable behaviour are made with alumina, zirconia, carbon, hydroxyapatite, or bioglass. Applications in medicine may become reality with the convergence of three distinct technologies: medical imaging, image processing and finally rapid prototyping of the ceramic implant such as bones and teeth prostheses.

Laser stereolithography (STL) represents the most common process for rapid prototyping but, up to now, it has been limited to the manufacturing of plastic materials. The shape and the dimensions of the parts are directly transferred from a three dimensional CAD system to the stereolithography equipment where a laser beam (usually from He–Cd or Ar laser) polymerises and solidifies a liquid resin layer by layer.

The multiphase system zirconia/alumina is an interesting technical ceramic with improved toughness with respect to pure alumina ceramics.[7–9] The optimum conditions are met when the included zirconia particles are large enough to transform their phase, but small enough to cause limited micro-crack development.[9]

The aim of this work is to demonstrate that standard STL equipment can be used to build green parts.

Therefore, the main objectives are:

- to use laser stereolithography for fabricating green bodies of ceramic structural components formulating photoreac-

* Corresponding author. Tel.: +39-0832-297321; fax: +39-0832-297525.
E-mail address: antonio.licciulli@unile.it (A. Licciulli).

0955-2219/$ – see front matter © 2004 Elsevier Ltd. All rights reserved.
doi:10.1016/j.jeurceramsoc.2003.12.003

tive suspension containing ceramic powders and resin with similar properties in terms of viscosity and UV reactivity to those of STL commercial resins;
- to use a liquid organometallic zirconate with the required reactivity and viscosity for a STL process and with the ability to act as ceramic precursor thus increasing the solid yield and improving the structural properties of the ceramic.

2. Experimental

2.1. Materials

The liquid reactive phase of the suspension is the zircon acrylate NZ39, neopentyl(diallyl)oxy, triacryl zirconate from KEN REACT whose chemical structure is given in Fig. 1.

The NZ39 is loaded with the alumina powder AES-23 from Sumitomo (AES stands for Alumina Easy Sintering), with a density, after sintering at 1600 °C, of 3.77 g/cm^3, a mean particle size of 1.8 μm, a surface area of 0.42 m^2/g and a linear shrinkage on sintering of about 16%. In every formulation 1-hydroxy-cyclohexyl-phenyl-khetone Irgacure 184 from Ciba, as photoinitiator, is added (3 wt.% with respect to zirconate). Suspension preparation is done using a ball mill equipped with alumina balls and vessels, using the zirconate resin as the liquid medium. The volume percentage of the resin was varied in the range from 40 to 60%, as reported in Table 1.

2.2. Stereolithographic set-up

The STL experimental set-up is represented in Fig. 2. It is composed of:

(i) A He–Cd laser, from Omnichrome series 3056, with 16 mW/mm^2 specific power, emitting at 325 nm, and with a beam diameter of 0.2 mm;
(ii) A scanning mirror which drives the laser beam on the suspension surface;

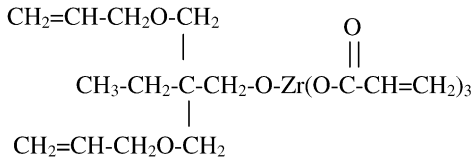

Fig. 1. Chemical structure of NZ39.

Table 1
Composition of the ceramic suspensions

Code	Organic	Al_2O_3 (vol.%)
SL5170	Commercial resin used as reference	–
Z001	Zirconate + 3% Irgacure 184	–
B006	Zirconate + 3% Irgacure 184	50
B011	Zirconate + 3% Irgacure 184	40

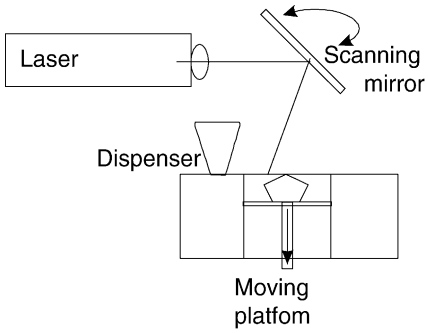

Fig. 2. Sketch of the experimental STL apparatus.

(iii) A software which controls the scan system allowing the construction of rectangular parts scanning the vat surface along parallel lines. The parameters which can be controlled are the scanning direction, the dimension of the part, the scan speed and number of scans per unit width. The energy per unit area was controlled by properly setting the last two parameters;
(iv) A moving platform with manual control, which can move downward to build a new layer after suspension re-filling. A recoating unit keeps constant the resin level moving in the plane parallel to the resin surface. The speed of the recoater determines the shear rate acting on the suspension, as will be explained later. Typically the ceramic parts have been obtained by laser exposure of each layer to an energy dose of 10 mJ/mm^2. The thickness of each layer has been chosen to be 0.1 mm, resulting in a good compromise between cure depth, processing times and shape tolerances.

2.3. Binder burnout and sintering

After manufacturing by STL, the green ceramic structures were converted to ceramic components by burning out the organic and sintering. The part was heated to 150 °C at 2 °C/min and held for 1 h to postcure the acrylates which may not have been fully reacted with the laser exposure.

The temperature was then increased to 500 at 200 °C/h and held for 1 h to burnout the binder. The samples were then heated at 300 °C/h to 1550 °C, and held at that temperature for 90 min. After cooling down, the specimens for mechanical tests were ground with abrasive paper to reduce the surface roughness.

2.4. Characterisation

The suspensions have been characterised in terms of UV reactivity and viscosity. The green components were studied with thermal analysis, and the mechanical properties and microstructure of sintered parts were analysed.

A differential scanning calorimeter (DSC) Perkin-Elmer DSC-7 was used to study the curing behaviour of the resin in air at 25 °C. The DSC is modified to irradiate the sample

using transparent quartz windows. The samples were irradiated with a 300 W Xenon lamp Cermax LX 300, limited to a wavelength interval of 325 + 4 nm using a monochromator, in order to simulate the irradiation band of a He–Cd laser beam. Lenses and mirror were used to focus the lamp light on the sample. The light intensity is modulated using a series of neutral filters and is measured at the beginning of each experiment using a power meter OPHIR PD2A. The heat generated by the light is negligible at the used UV wavelength. Data were recorded from the instrument, and the exothermal heat flow was subtracted by the baseline value BL.

The viscosity of suspensions at 25 °C is measured using an Ares (Rheometric Scientific) instrument, a cone and plate geometry is used to evaluate viscosity at shear rate between 0.1 and 100 s^{-1}.

Thermogravimetry (TGA) was used to study the behaviour of the green samples during pyrolysis of the organic binder and sintering with a Netzsch STA 409 analyser.

Microstructural analyses were performed with scanning electron microscopy and X-ray diffraction using a scanning electron microscope (SEM) Philips PW1880 powder diffractometer with q–2q geometry.

Three point bending tests were performed using a Lloyd LR5K instrument, on 50 mm × 5 mm × 3 mm sintered ceramic bars according to UNI EN 843. In this way, for each specimens, the Young's modulus and the strength were measured.

3. Results and discussion

The organometallic zirconate, is a known coupling agent used to chemically bond inorganic and organic surfaces. Due to its coupling action it was found very effective to disperse the inorganic alumina powders, characterized by an hydroxyl rich surface. The prepared suspensions did not show any precipitation or powder segregation nor granule formation. One problem encountered was the limited suspension lifetime; after approximately one month a significant viscosity increase was noticed. The limited lifetime of the suspension is attributed to the ongoing condensation reactions of the alkoxide functionality of the zirconate, resulting in a cross linking action among particles and monomers.

The reactivity of the monomer is due to the polymerisation of the acrylate groups induced by the UV irradiated photoinitiator. This has been studied with the special DSC set-up described in the previously. The heat flow signal was integrated, in order to estimate the value of the heat of reaction developed as a function of time.

$$\Delta H(t) = \int_0^t (\dot{q}(t) - \mathrm{BL})\mathrm{d}t$$

From this, the value of the degree of reaction is defined as the ratio of the partial heat of reaction developed during a DSC experiment to the total heat at the end of the reaction.

$$\alpha = \frac{\Delta H(t)}{\Delta H_{\mathrm{tot}}}$$

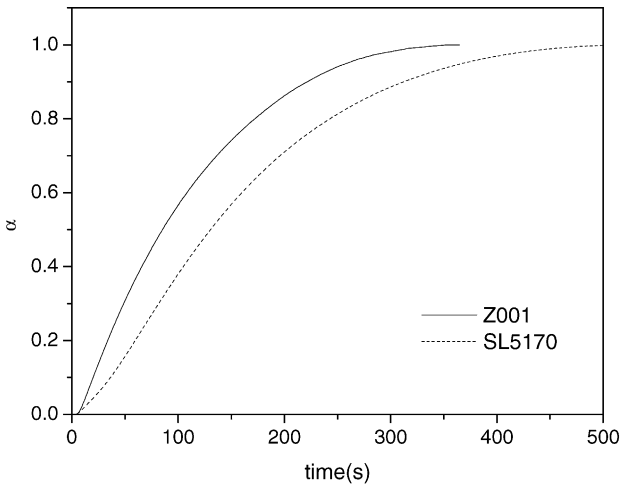

Fig. 3. Plot of the degree of reaction vs. time of different commercial resins and formulations for green pre-ceramic.

The zirconate resin shows a better reactivity compared with the commercial SL5170 resin, commonly used in the process of stereolithography (Fig. 3). The time to reach full conversion is about 5.5 min, against 8 min for the commercial resin. This means that the organometallic zirconate alone can be cured with a lower dose of energy than the commercial STL resin.

The reactivity of a STL resin is characterised by two parameters relating the cure depth (C_d) with the energy dose at the vat surface (E_o):[1]

$$C_d = D_p \ln \frac{E_0}{E_c} \quad (1)$$

where the working parameters D_p and E_c, are the penetration depth and critical energy respectively and the cure depth represents the thickness of gelled resin. E_c is the minimum value of energy needed to promote polymerisation, while D_p is the gelled thickness when $E_0 = E_c e$.

The working parameters of suspensions are calculated by measuring the thickness of single layer specimens obtained curing 1 cm square zone of the surface of the suspension at different values of E_o. A linear regression on experimental C_d values plotted as a function of $\ln(E_o)$ is used for the determination of D_p and E_c from the slope and the intercept respectively. The working curve is compared in Fig. 4 with that of SL5170, obtained using literature values of D_p and E_c.[10]

The experimental values of E_c and D_p are reported in Table 2.

A good stereolithography resin should have low values of E_c, in order to start the reaction with a low energy dose, and high values of D_p, in order to have higher cured thickness. As expected from DSC data, the higher reactivity of the zir-

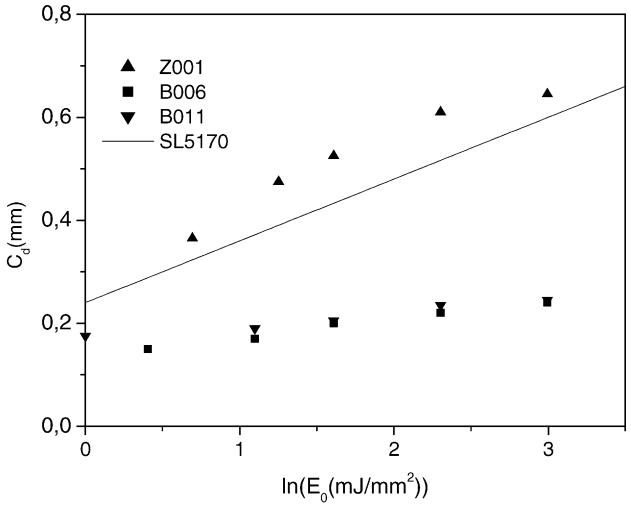

Fig. 4. Working curves for the ceramic suspensions compared with working curves of commercial STL resins.

conate lead to higher solidified thickness at a given energy dose (Fig. 4). The zirconate alone therefore, shows better reactive properties than the commercial one, especially concerning the value of E_c, which is lower. The addition of alumina powders results in lower values of D_p, because of the scattering of light from ceramic particles, whereas the influence on E_c is probably due to the reduced oxygen inhibition related with the lower surface exposed to atmosphere with increasing alumina content. In any case our formulations seem to have quite good reacting properties, and lead to sample parts without any curl distortions. A significant deviation from Eq. (1) is obtained at high energy doses; in fact, loading the zirconate with alumina significantly reduces the depth of penetration and is not possible to raise it above 200 mm. Rather it seems that saturation is reached most likely due to the light scattering from the surface and crystalline grain boundaries of the powder. The scattering from particles acts like a shield preventing light penetration in the underlying suspension. The thickness of cured layer of a suspension depends on several "hidden" parameters and the scattering theories of Rayleigh-Gans or Mie are not sufficient in estimating the dependence on particle size and concentration.[11] It has been found empirically[12] that the scattering yield depends on the particle size, on the ratio of the inter-particle spacing to the radiation wavelength and on the square of the refractive index difference between the different phases.

Nevertheless the penetration depth obtainable in the powder loaded zirconate is still satisfactory for a stereolithographic process. Since the penetration depth is inversely proportional to the resolution and finishing of the prototype, high penetration depth is not desirable. In most cases a layer thickness of 100 mm is preferred.

As stated above, the powder is well dispersed in the monomer thanks to the oxy-pentyl group of the NZ39 which is thought to undergo hydrolysis reactions with surface hydroxyls present on the ceramic powder. This reaction improves wetting and therefore a good dispersion is obtained. The viscosity of the suspension is an important parameter in STL. Ideal situation is to provide a low viscosity to let the resin level itself with gravity. Such a requirement is difficult to be fulfilled with highly solid loaded ceramic suspensions that behave like a Bingham liquid and display a yield stress point. Real situations therefore need at least good levelling and levelling by doctor blade treatment in the recoating phase. Viscosity versus shear rate measurements are reported in Fig. 5. Measurements were performed between 0.1 and 100 s^{-1} shear rate interval and showed that the viscosity of the suspension, at low shear rates, is much higher than that of the commercial resin, showing a Bingham like behaviour, (shear thinning). At higher shear rates, the difference decreases and at about 100 s^{-1} the two formulations have similar viscosities.

Since the values of shear rates applied on the resin during recoating are related to the speed of the recoating unit, the ceramic suspension can be used with proper selection of recoating bar speed as a function of cast resin thickness. In fact, the shear rate $\dot{\gamma}$ is related to the bar speed v and to the resin thickness through: $\dot{\gamma} = v/d$. In order to operate below the maximum allowable viscosity value corresponding to 5 Pa s a shear rate of 30 s^{-1} is needed. At the selected thickness of 100 μs, the speed of the recoater has consequently

Table 2
Working parameters for the different suspensions and resins

Code	E_c (mJ/cm^2)	D_p (mm)
Z001	7.6	0.12
SL5170	13.5	0.12
B006	2.25	0.03
B011	0.119	0.025

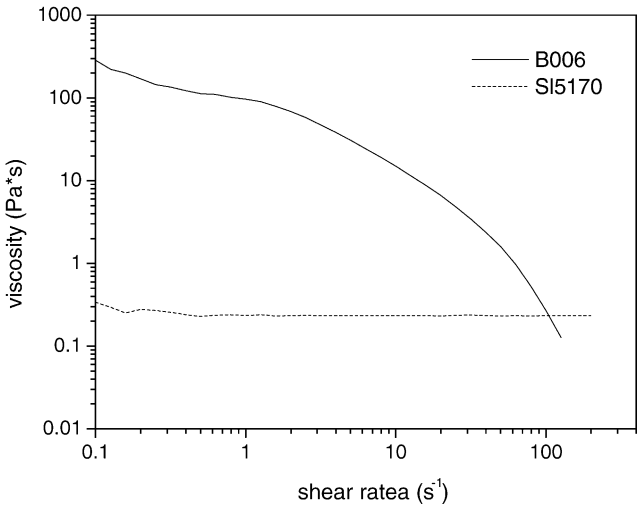

Fig. 5. Shear viscosity curve of B006 suspension compared with SL5170.

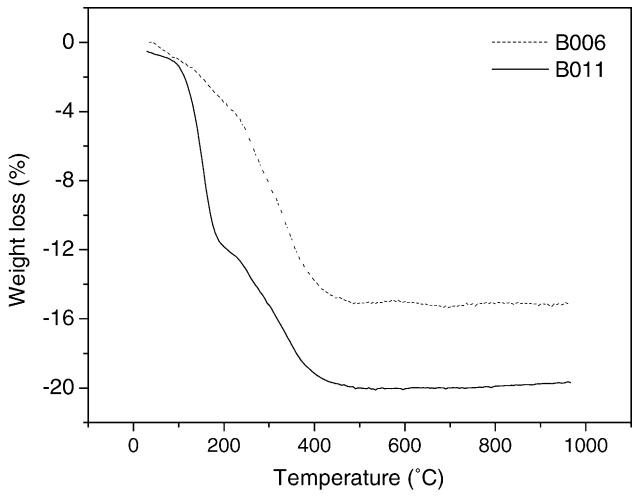

Fig. 6. Thermogravimetric analysis of ceramic suspension at different solid loading.

to be set at least at a value of 3 mm/s (maximum allowed speed on commercial SLA being 30 mm/s). The same viscosity of SL5170 is obtained operating the recoater bar at 10 mm/s. It is then confirmed that the suspension as far as it concern its rheological properties can be used in commercial stereolithographic apparatus.

TGA was used to identify the temperature intervals where pyrolysis and sintering take place and to evaluate the solid yield of the ceramic suspensions.

An additional solid residue at the end of the resin burn out is attributed to the formation of ZrO_2. This is evident in Fig. 6, where it can be seen that the weight loss is about 20 and 8.5% by weight for the suspension filled with 40 and 50% by volume of alumina. These values are much higher than the values achievable with suspensions not containing resin characterized by solid yield upon pyrolysis. Accounting only for alumina powders, a weight loss of about 28% for B011 and 20% for B006 should be observed (Fig. 6).This is especially important during sintering, when the presence of a higher solid residual makes it possible to minimize the effects of shrinkage and to obtain higher density products.

Following the indications of TGA experiments, the resin burn out between 100 and 500 °C must be very slow, because in this phase the gas evolved can destroy the samples. The overall thermal treatment has then been divided into the three steps described in the experimental section.

The diffraction spectrum of a sintered specimen is reported in Fig. 7. The α-Al_2O_3 peaks are dominant but monoclinic (m-ZrO_2) and tetragonal ZrO_2 (t-ZrO_2) peaks are also present. Their intensity is very weak and this indicates that $ZrO_2$is present as a minor phase. By evaluating the full width at half maximum and using the Scherrer equation,[13] a rough estimation of the size of the zirconia crystallites was obtained. It was found that $D = 24.6$ nm for m-ZrO_2, $D = 54.9$ nm for t-ZrO_2. XRD studies confirm a very interesting result: as a consequence of pyrolysis and organic burn out the zirconate compound decomposes and forms zirconium oxide that remains separated from alumina phase and crystallizes forming a submicron, well dispersed phase. Since no stabilization by cation addition (Y, Ca) has been done, zirconia is supposed to undergo the distorsive polymorphic transformations from cubic to tetragonal to monoclinic during cooling. The presence of unconverted tetragonal phase can be attributed to the high compressive stress exerted by the alumina matrix to the ZrO_2 particles.

Three point flexural tests are reported in Fig. 8. The strength is about 175 MPa, whereas the flexural modulus is 193 GPa. The low values obtained for modulus and strength (about half of that for traditionally sintered alumina powders) can be attributed to poor adhesion between adjacent

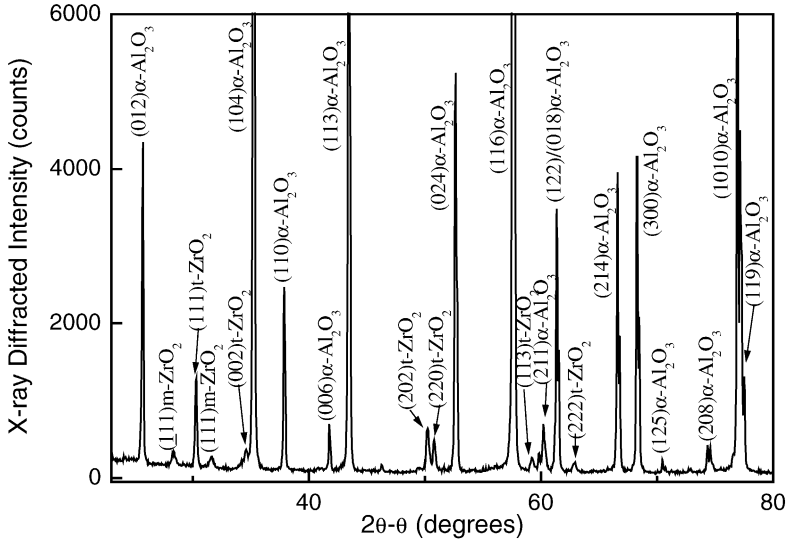

Fig. 7. X-ray diffraction analysis for ceramic sintered part built from B006 suspension.

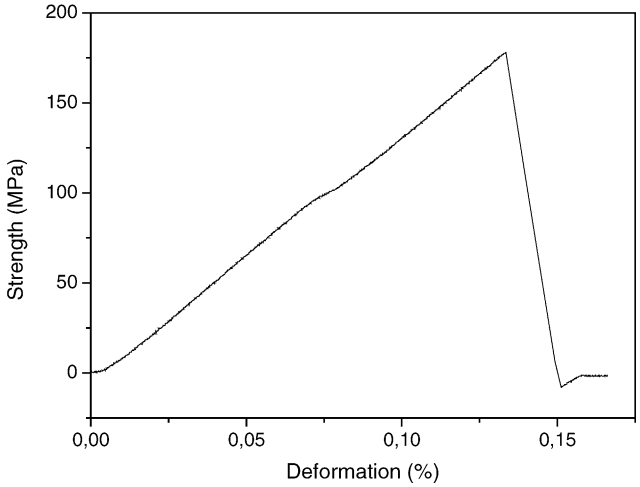

Fig. 8. Stress–displacement curve obtained from a three point bending test performed on a ceramic sample built from B006 suspension.

layers and to the high porosity of the ceramic components. In facts, the bulk density value is 3.33 g/cm^3, compared to a maximum value of 3.77 g/cm^3 of the alumina powder used reported by Sumitomo technical sheets.

An extended SEM characterisation has been performed on sintered samples.

An image obtained from SEM analysis on a fractured surface is reported in Fig. 9, it is showing only a limited layer separation near to the upper right corner. Despite some porosities are still present, the sample does not exhibit evident delamination as it was found in alumina/silica multiphase systems previously prepared.[14]

Fig. 10 shows the presence of zirconia particles in the alumina matrix, and also it shows the bimodal distribution of alumina grains that results from the peculiar alumina powders used.

The bimodal particle distribution is a key feature of this alumina; it makes AES23 particularly suitable for the stereolithographic process; in fact, low viscosity in the suspension, easy particle packing and low shrinkage after sintering. Due to the large grain size and to a sintering temperature kept below 1550 °C during sintering, a full densification was not obtained leading to above mentioned bulk density.

Fig. 11 shows that zirconate creates particles substantially smaller than the grains of the alumina matrix. These particles are located, after sintering, on grain boundaries of alumina particles. It is also likely, evaluating this figure, that zirconia acts as a grain growth inhibitor in the alumina matrix, allowing an improvement of mechanical properties of the ceramic components. Similar results in terms of uniform distribution and location at the grain boundary of zirconia grains were obtained by other authors through liquid infiltration of alumina presintered samples in zirconium propoxide.[15]

The grain size distribution of zirconia submicron particles has been evaluated from the SEM analysis (Fig. 12). Generally, the particles are relatively uniform in size distribution, but not in shape (they do not have perfectly spherical geometry). The particles are essentially in a random configuration

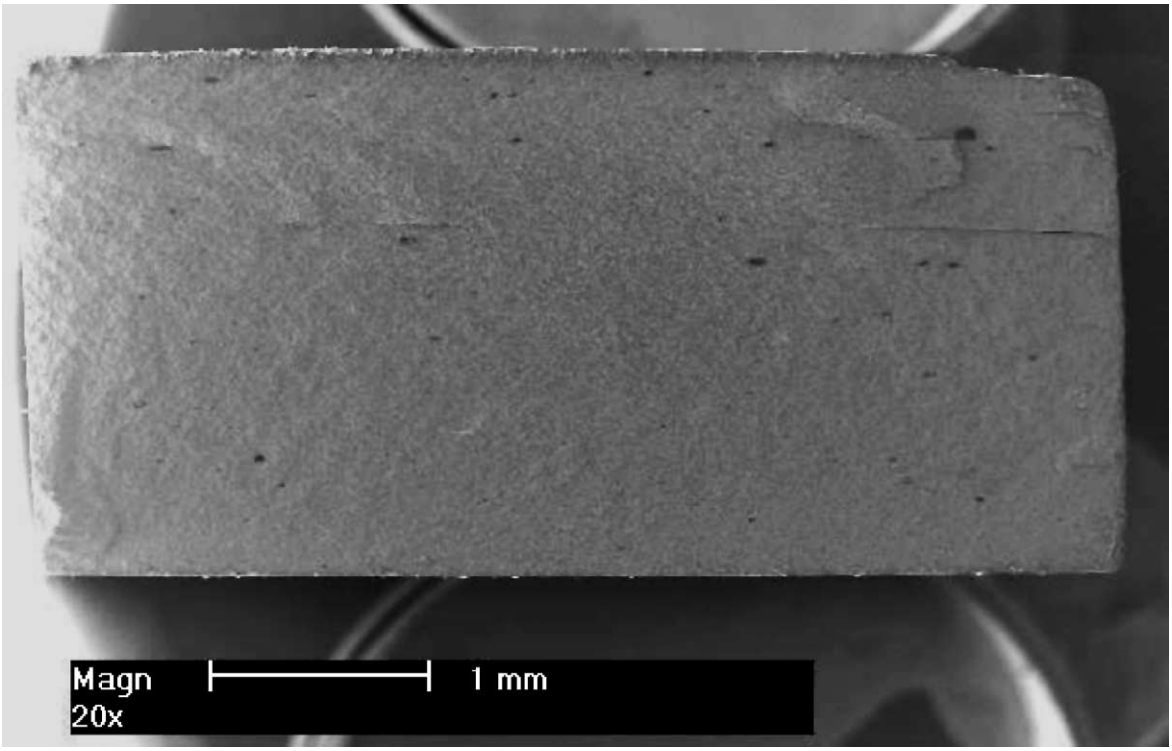

Fig. 9. Image from SEM analysis of a fracture surface, which show no delamination at the interface between adjacent layers.

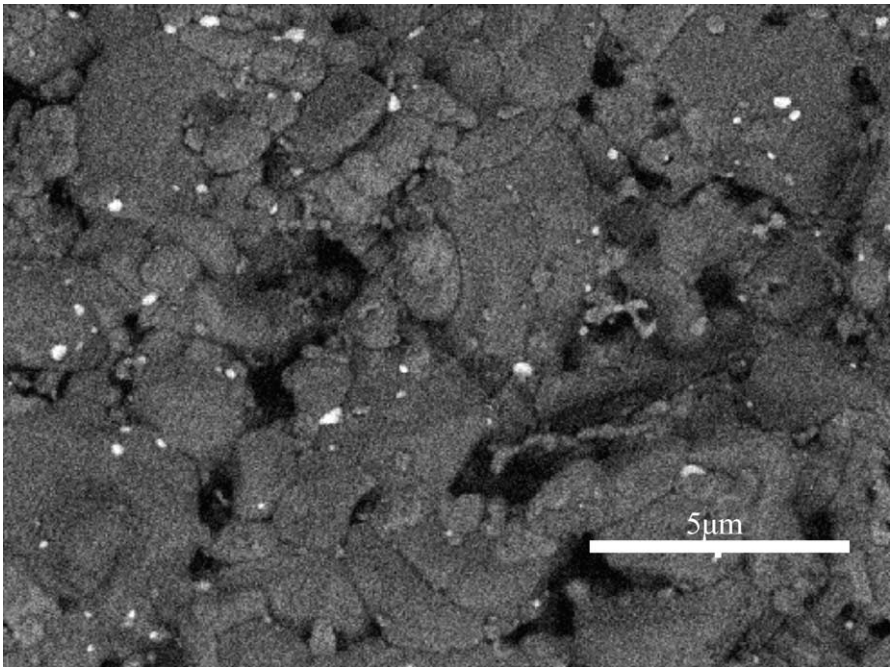

Fig. 10. Unpolished section evidencing the zirconia phase located at the grain boundaries of bimodal distributed alumina particles.

with resulting pore size varying from 20 nm to 1 μm. The nano-sized ZrO_2 particles are homogeneously distributed, without agglomerates, at the alumina grain boundaries and therefore minimal microstructural flaws. Likewise, due to the small size of the zirconia grains and their narrow grain size distribution, it is possible to retain a larger amount of tetragonal zirconia grains in the alumina matrix and this contributes to the transformation toughening mechanism operating in this composite.[16]

Higher toughness and improved mechanical properties, lower susceptibility to stress assisted corrosion by water or body fluid may be expected if strong bonding occurs between the alumina and zirconia particles and if no microcracks are present after processing. It has been reported that 10% by volume of zirconia in the alumina matrix is a good compromise to reach good toughening effect without decreasing the strength due to the high microcrack density.[17] In our case, TGA experiments and stoichiometric

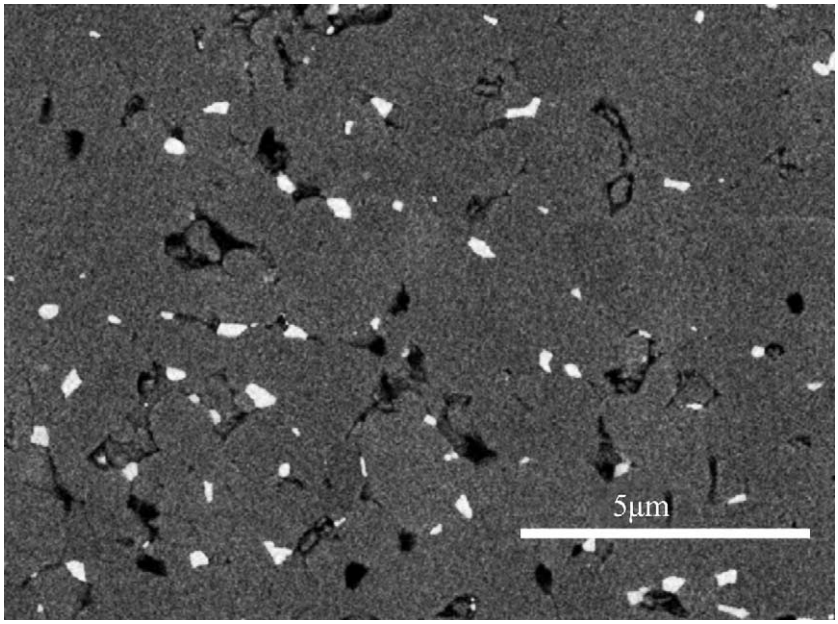

Fig. 11. Polished section evidencing the zirconia phase located on the grain boundaries of Al_2O_3 particles.

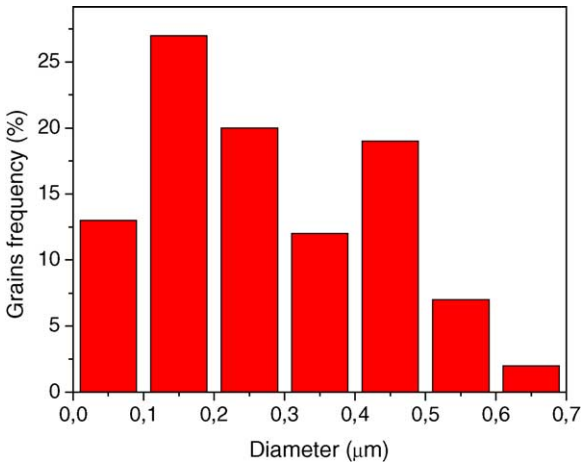

Fig. 12. Submicron zirconia distribution.

calculations indicate that the zirconia content in the sintered specimen is about 8 vol.% for B011 that is the sample with the highest initial zirconate volumetric percentage (60 vol.%).

The average size of zirconia grains is about 200 nm. As it is reported in the literature,[18] this value is low enough to allow the existence of the tetragonal zirconia in the alumina matrix even at room temperature. Thus, it was possible to obtain nano-sized particles in the range from the critical size for spontaneous transformation after sintering, $D_c = 0.1$ mm, (above which there is no reinforcement) to the critical size for transformation during crack growth, $D'_c = 0.6$ mm, (below which there is no crack induced transformation, thus no reinforcement).[18–21]

In order to demonstrate that complex shape can be easily produced using our STL process an alumina nozzle was first designed with CAD and then manufactured. The CAD design and the sintered ceramic nozzle are reported in Fig. 13.

4. Conclusions

Photoactivated ceramic suspensions have been prepared from alumina powder and organometallic zirconate. The ceramic suspensions have been studied carefully, in particular their photoreactivity and their viscosity is important in the forming process, their thermal behaviour and ceramic content are important for the sintering and for the structural properties.

It is confirmed that ceramic structural components can be designed and fabricated by stereolithography from these photoactivated ceramic suspensions. In this work a promising zirconate monomer as ceramic precursor was successfully used.

The organometallic zirconate was very effective for the powder dispersion and showed satisfactory reactivity even at high powder loading. Another interesting effect was the formation, upon pyrolysis and sintering, of a multiphase system of the type alumina zirconia. Zirconia is present in tetragonal and monoclinic crystalline form, as revealed by XRD.

Some points still need to be optimised i.e. the time durability of the suspension that is presently limited to approximately a month and the residual porosity due to the starting powder selected.

Mechanical properties, i.e., strength and modulus are quite good but still don't reach what is found in the literature with other forming processes. More likely the difference are due to the still high residual porosity, not less than 10% and to the low level of surface finishing. A more detailed investigation is required for the correlation of the zirconia segregated phase and the toughening mechanisms that can be achieved.

Acknowledgements

The Italian Ministry of Scientific and Technological Research is acknowledged for the financial support of the project P11 "Applicazioni di tecniche di prototipazione e

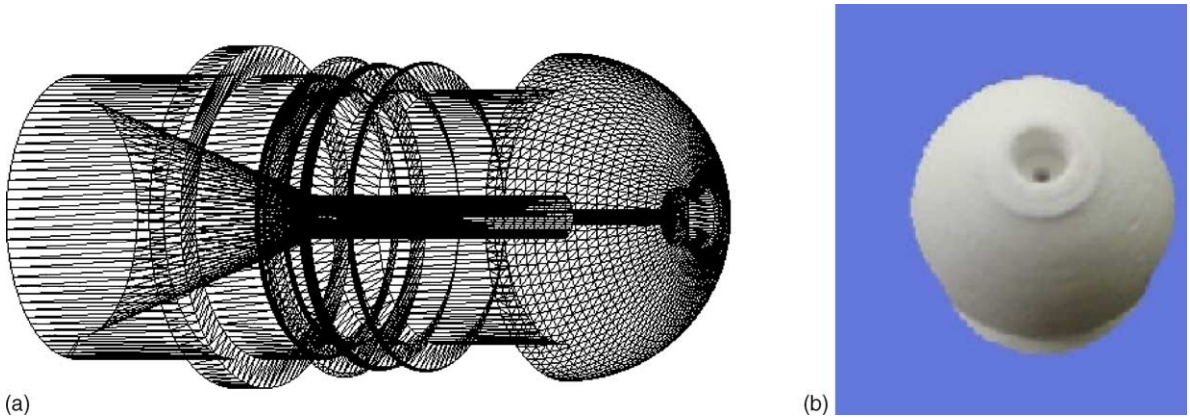

Fig. 13. CAD project of ceramic nozzle (a) ceramic nozzle produced with STL (b).

progettazione allo sviluppo di componenti industriali con materiali innovativi". Dr. B. Valli is also acknowledged for his technical support. Dr. S. Tundo of CNR IMM is acknowledged for her contribution in SEM analysis.

References

1. Jacobs, P. F., *Rapid Prototyping and Manufacturing*, SME, Dearborn, USA, 1992.
2. Greco, A., Licciulli, A. and Maffezzoli, A., Stereolithography of ceramic suspensions. *J. Mater. Sci.* 2001, **36**, 99–105.
3. Brady, G. A. and Halloran, J. W., Differential photo-calorimetry of photopolymerizable ceramic suspensions. *J. Mater. Sci.* 1998, **33**, 4551.
4. Cai, K., Guo, D., Huang, Y. and Yang, J., Solid freeform fabrication of alumina ceramic parts through a lost mould method. *J. Eur. Ceram. Soc.* 2003, **23**, 921–925.
5. Waller, D. J. and Safari, A., Piezoelectric lead zirconate titanate ceramic fiber/polymer composites. *J. Am. Ceram. Soc.* 1992, **75**, 1648–1655.
6. Marcus, H. L. and Bourell, L., Solid freeform fabrication. *Adv. Mater. Process.* 1993, **9**, 28–35.
7. Garvie, R. C. and Gross, M. F. *J. Mater. Sci.* 1986, **21**, 1253–1257.
8. Stevens, R. and Evans, P. A. *Br. Ceram. Trans. J.* 1984, **83**, 28–31.
9. Stevens, R., *Zirconia and Zirconia Ceramics, Pub. 113*. Magnesium Elektron Inc., Flemington, NJ, 1986.
10. CIBA-GEIGY, *Technical Data Sheet*.
11. Vera, M. U. and Durian, D. J., The angular distribution of diffusely transmitted light. *Phys. Rev. E.* 1996, **53**, 3215–3224.
12. Griffith, M. L. and Halloran, J. W., Freeform fabrication of ceramics via stereolithography. *J. Am. Ceram. Soc.* 1996, **79**(10), 2601–2608.
13. Sun, X. W., Wang, L. D. and Kwok, H. S., Improved ITO thin films with a thin ZnO buffer layer by sputtering. *Thin Solid Films* 2000, **360**, 75–81.
14. Licciulli, A., Greco, A. and Maffezzoli, A., Development of a pre-ceramic suspension for free form fabrication of ceramic parts by stereolithography. *Ind. Ceram.* 2000, **20**, 97–99.
15. Galusek, D. and Majiling, J., Preparation of Al_2O_3–ZrO_2 ceramics by infltration processing. *Ceram. Int.* 1995, **21**, 101–107.
16. De Aza, A. H. *et al*., Crack growth resistance of alumina. *Biomaterials* 2002, **23**, 937–945.
17. Claussen, N. *J. Am. Ceram. Soc.* 1976, **59**(1/2), 49–51.
18. Heuer, A. H., ed., Advances in ceramics science and technology of zirconia. *Am. Ceram. Soc.* 1981, **3**, 137–163.
19. Claussen, N. *J. Am. Ceram. Soc.* 1976, **59**(1/2), 49–51.
20. Messing, G. L. and Kumagai, M. *J. Am. Ceram. Soc.* 1989, **72**(1), 40–44.
21. Srdic, V. V. and Radonjic, L. *J. Am. Ceram. Soc.* 1997, **80**(8), 2056–2060.